Dist: A

REPORT DOCUMENTATION PAGE

Form Approved
OMB No. 0704-0188

1. AGENCY USE ONLY (Leave blank)	2. REPORT DATE	3. REPORT TYPE AND DATES COVERED
	2/10/95	05/01/94 - 09/30/94 Final Technical

4. TITLE AND SUBTITLE

Ceramics Derived from Metallic Precursors

5. FUNDING NUMBERS

F49620-94-1-0099

61102F
2303/BS

6. AUTHOR(S)

Dr. Donald R. Uhlmann

7. PERFORMING ORGANIZATION NAME(S) AND ADDRESS(ES)

Department of Materials Science and Engineering
College of Engineering and Mines
The University of Arizona
Tucson, Arizona 85721

8. PERFORMING ORGANIZATION REPORT NUMBER

AFOSR-TR- 95 - 0105

9. SPONSORING/MONITORING AGENCY NAME(S) AND ADDRESS(ES)

AFOSR/~~NC~~ NL
110 Duncan Avenue, Suite B115
Bolling AFB, DC 20332-0001

Maj Thomas E. Erstfeld

10. SPONSORING/MONITORING AGENCY REPORT NUMBER

11. SUPPLEMENTARY NOTES

12a. DISTRIBUTION/AVAILABILITY STATEMENT

Approved for Public Release: Distribution unlimited

12b. DISTRIBUTION CODE

A

13. ABSTRACT (Maximum 200 words)

During the five months covered by this grant, our research on the program was principally focused on two areas: These are: (1)use of silylated laser dyes in solid state hosts; and (2) optical properties and surface patterning of polyceram materials. Progress in each of these areas will be summarized in the following sections.

14. SUBJECT TERMS			15. NUMBER OF PAGES
			16. PRICE CODE
17. SECURITY CLASSIFICATION OF REPORT	18. SECURITY CLASSIFICATION OF THIS PAGE	19. SECURITY CLASSIFICATION OF ABSTRACT	20. LIMITATION OF ABSTRACT
Unclassified	Unclassified	Unclassified	UL

FINAL REPORT

submitted to

AIR FORCE OFFICE OF SCIENTIFIC RESEARCH

by

University of Arizona

on

Ceramics Derived From Organo-Metallic Precursors

(Grant F49620-94-1-0099)

during the period

5/1/94 - 9/30/94

Principal Investigator: Professor D. R. Uhlmann

I. INTRODUCTION

During the five months covered by this grant, our research on the program was principally focused on two areas. These are: (1) use of silylated laser dyes in solid state hosts; and (2) optical properties and surface patterning of polyceram materials. Progress in each of these areas will be summarized in the following sections.

II. Silylated Laser Dyes

The past decade has seen great interest in producing a solid-state organic gain medium. Since dye/solvent lasers require pumping systems, and have limited lifetimes due to photo-decomposition and chemical instability, solid state organic media appear attractive for tunable solid state lasers, especially in the visible.

Laser dye molecules have been doped into both polymers and inorganic glasses. Polymer hosts suffer significant photodegradation due to free radical formation of the dye molecules . Inorganic hosts appear more attractive because they have high laser damage thresholds. Because of the limited temperature stability of organic lasing dyes, using a low temperature sol-gel process is attractive for incorporating organic molecules within an inorganic host. Numerous lasing dyes, such as rhodamines and coumarins, have been incorporated within sol-gel hosts of silica, alumina, and organically modified silica (Polycerams). Caging lasing dyes within a sol-gel host has shown improved (but still inadequate) photostability and has permitted high dye concentrations without undesirable dye aggregation. Dye/host interactions could provide for greater tuning of the fluorescence, improved photostability, reduced photodegradation, and even improved quantum efficiency of the fluorescence.

A number of silylated dyes, such as silylated Disperse Red 1, silylated para-nitroaniline, and silylated dinitroaniline (TDP), have been incorporated in sol-gel matrices for nonlinear optic applications. Silylated dyes have been used to bond the dye chemically within the matrix.

The use of silylated active molecules seems attractive for laser dye/sol-gel nanocomposites. Increase in the effective molecular rigidity and possible reduction in aggregation could provide for improved quantum yield by limiting nonradiative transitions. Also, it is hypothesized that improved photostability may be achieved due to further reduction of both vibrational and rotational modes of energy dissipation and greater dye isolation. Isolation of the dye molecules limits the interaction between the molecules reducing intersystem crossing to the triplet states and hence reducing decomposition.

The present study has investigated the effects of bonding a number of fluorescent dyes within a sol-gel matrix. A Coumarin 4 (Coum) laser dye was chosen because it has an -OH group which was readily functionalizable to form a silylated dye. Unfunctionalized Coum has been successfully incorporated in sol-gel matrices and its fluorescent properties have been well characterized. A number of silylated dyes have been synthesized in our laboratory with various linkages and degree of functionality. The structure of these dyes are shown in Fig. 1. Result for

all the dyes have and are currently being investigated. In the following report, concentration has been placed on Coum and DerCoum dyes.

A. Synthesis of DerCoum

7-hydroxy-4-methylcoumarin (Coumarin 4) (Aldrich Chemical Company) was recrystallized and reacted with 3-isocyanatopropyltriethoxysilane (Huls) to obtain O-4-methylcoumarinyl-N-[3-(triethoxysilyl)-propyl]carbamate (derCoum) as shown in Fig. 2. The reaction was carried out in tetrahydrofuran (THF) with a tin catalyst and was monitored by FTIR (Perkin-Elmer 1725x). During the formation of the derCoum, the isocyanate peak (2290 cm^{-1}) disappeared and the urethane peak (1765 cm^{-1}) increased. DSC (Perkin-Elmer DSC-7) also confirmed formation of derCoum by indicating a large change in the melting point, 192 C for Coum and 95 C for derCoum.

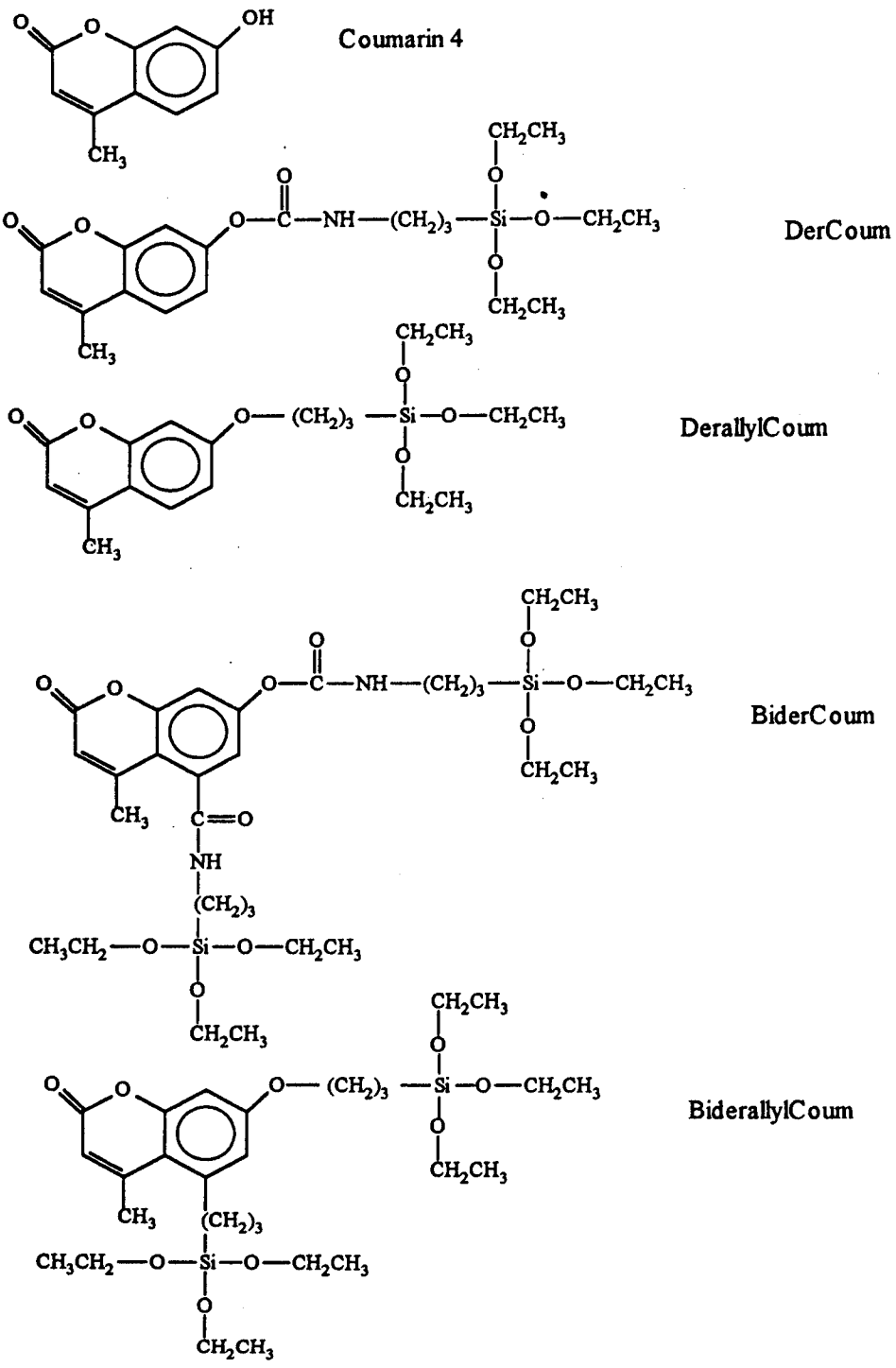

Fig. 1: Structure of Coum and Silylated Coumarins.

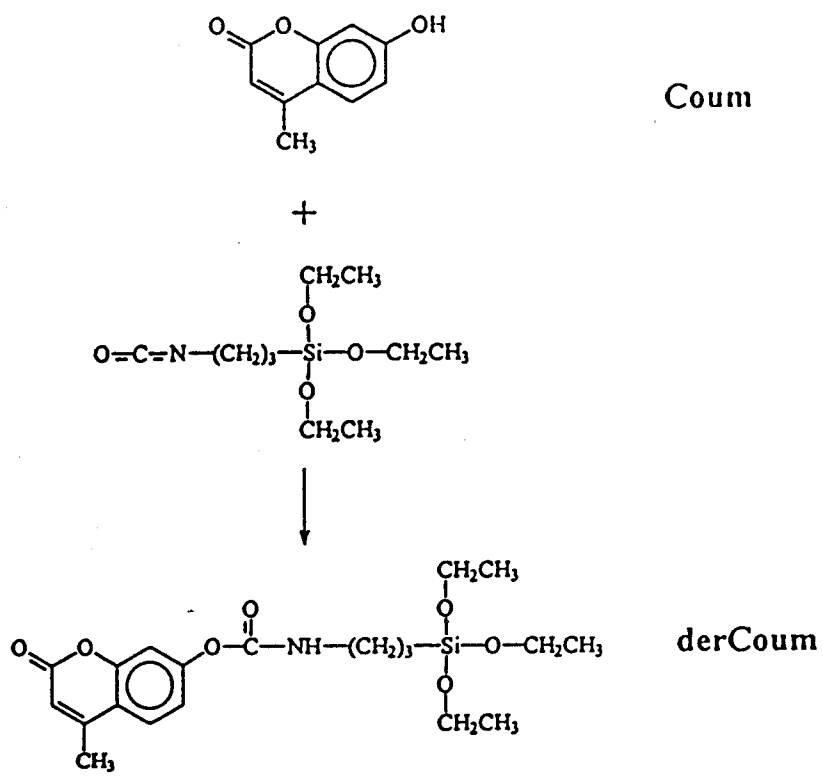

Fig. 2: Synthesis of DerCoum.

B. Preparation of Sol-Gel/Dye Xerogels

DerCoum and Coum were doped at various concentrations in sol-gel derived silica to form thin films. Typically, tetramethoxysilane (TMOS) and H_2O (acidified to 0.15 M HCl) were mixed in a glass vial at a TMOS:H_2O molar ratio of 1:4. Initially, the H_2O was insoluble within the TMOS, but rapid hydrolysis produced a miscible solution within a few minutes. Separately, the dye was dissolved in MeOH. DerCoum was more soluble than Coum in the solvent. Additional H_2O was added with derCoum solutions at a derCoum:H_2O molar ratio of 1:3. The two

solutions were mixed, resulting in a solution with a desired TMOS:dye molar ratio. The solids:solvent ratio of the final solution was maintained at a 1:2 weight ratio for all solutions. The pH of the solutions ranged from 1.8-2.2 depending on the dye concentration. After aging for 24 hrs, the solutions were passed through 0.8 μm filters and spin coated on pre-cleaned microscope slides (Gold Seal) at 2000 rpm for 20 sec. The films were dried at 125 C for 48 hrs in vacuum. All films were about 0.5 μm as measured with a Dektak II profilometer. All derCoum doped films were transparent, whereas at high concentrations, Coum-doped films appeared slightly cloudy due to crystallization of the Coum dye.

C. FTIR SPECTROSCOPY

The degree of bonding of the silylated dye to the matrix greatly depends on the reactivity of each of the precursors. In order to encourage dye-silica bonding as opposed to dye-dye bonding, it is worthwhile to match the reaction rates of the dye with the other precursors. It was found that the silylated dyes are the slower reacting species when compared with the other silicon alkoxides. Fourier Transform Infrared (FTIR) Spectroscopy is a useful technique for monitoring the rate of hydrolysis. The degree of hydrolysis was monitored by observing a decrease in the H_2O absorptions (vibrational band at 3570 cm^{-1}, molecular bending

band at 1647 cm^{-1}). Reactions used for FTIR analysis were conducted in THF to avoid the large -OH bands that are observed in alcohol solvents. To ensure quantitative analysis of reaction rates, a CaF_2 sealed cell with a 0.1 mm teflon spacer was used to ensure a constant path length and to prevent solvent evaporation.

The results of this kinetic investigation are shown in Fig. 3. The mono-functionalized dyes (DerCoum, DerAllylCoum) hydrolyzed slower than its bi-functionalized counterpart (BiDerCoum and BiDerAllylCoum, respectively). Also, the dyes with propyl linkages between the dye and silicon alkoxide hydrolyzed faster than the dyes with a urethane linkage.

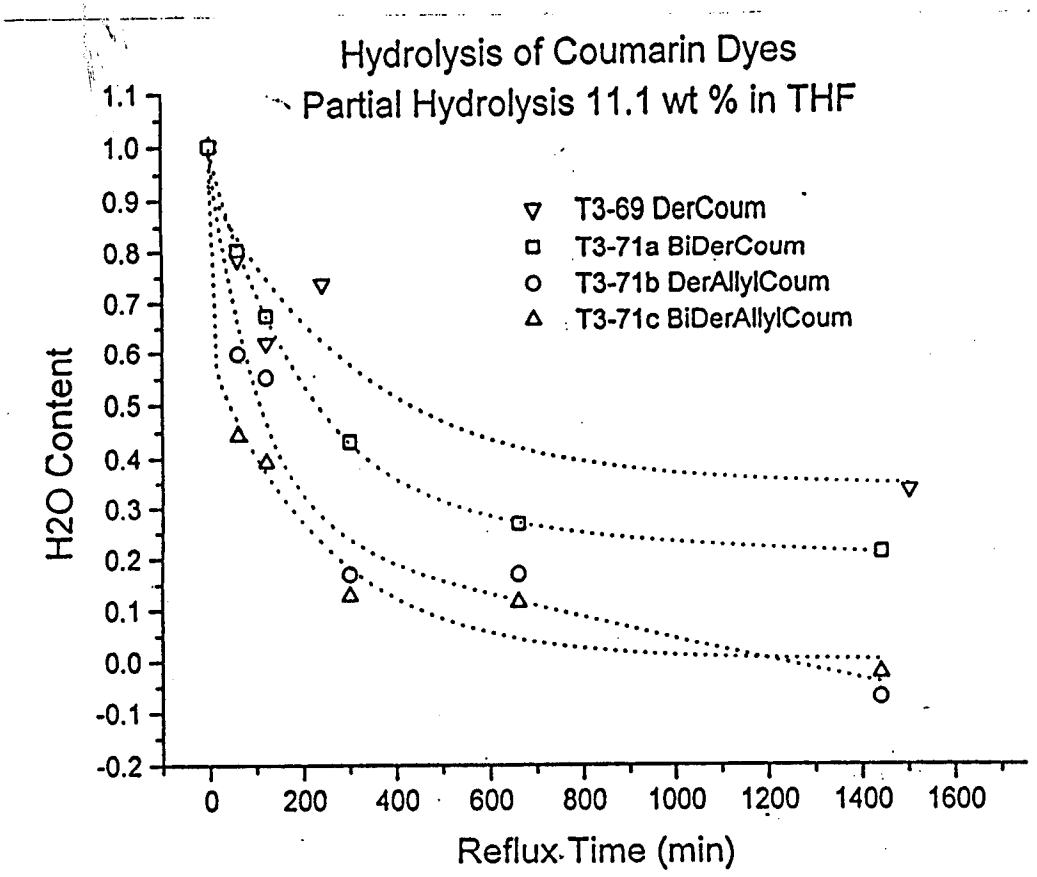

Fig. 3: Hydrolysis of Silylated Coumarin Dyes

D. Absorption and Fluorescence Spectra

The samples were pumped at normal incidence with a N_2 laser (Photochemical Research Associates LN1000) at 337 nm with a pulse rate of 6 Hz. The fluorescence spectra were measured using the arrangement shown schematically in Fig. 4. A filter was placed in front of the optical multichannel analyzer (OMA) (EG&G) to block off the 337 nm light. The spectrometer of the OMA was calibrated with a mercury light source.

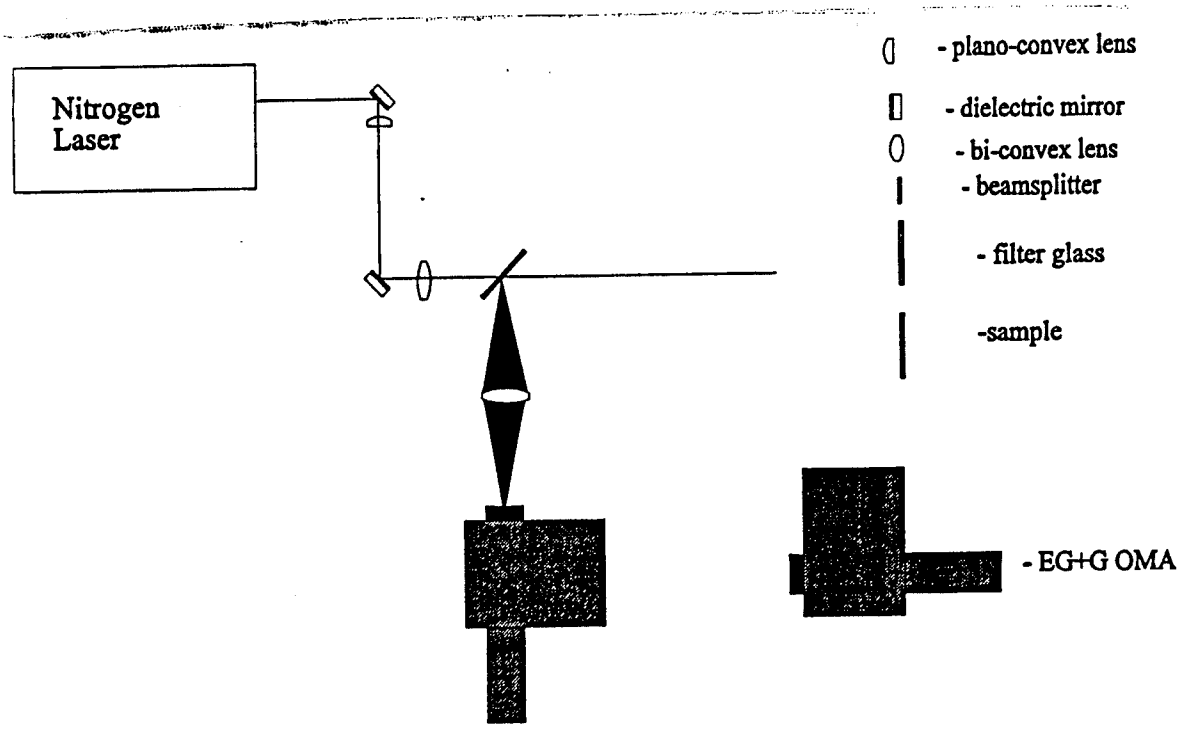

Fig. 4: Schematic of fluorescence measurement apparatus.

Numerous chemical forms of Coum are known depending on its environment (e.g., pH) in solvent and sol-gel hosts. Three of the ground state forms - neutral, anionic, and cationic - absorb at 320, 365, and 340 nm, respectively, and fluoresce at 400, 455, and 420 nm, respectively. The zwitterionic exciplex form fluoresces at 475 nm. The structure of chemical forms of Coum are illustrated in Fig. 5.

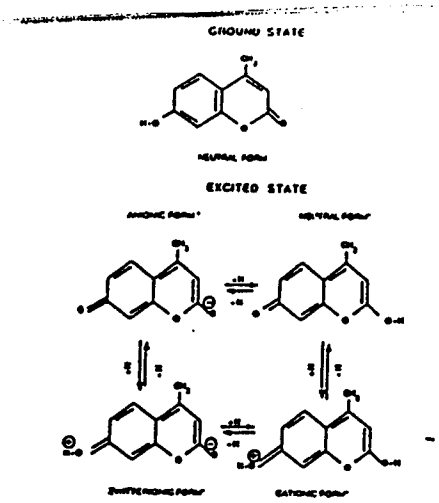

Fig. 5: Structure of different forms of Coum.

Fig. 6 shows the absorption and the fluorescence curves for Coum and derCoum dyes at approximately 10^{-5} moles/L in MeOH adjusted to a pH of 2.0 by the addition of HCl. Both of the dyes have very similar absorption spectra with a maximum at 319 nm, indicating the presence of the neutral ground state. The fluorescence of both dyes was also very similar. Multiple fluorescence emission was observed. This is attributed to the presence of the neutral, anionic, and zwitterionic forms in the excited state.

Blue fluorescence was observed in all the dye doped films. The absorption and fluorescence spectra of Coum and derCoum films at 0.01 M appear very

similar (Fig. 7). Both absorb near 320 nm and fluoresce in the 430-460 nm range, but the absorption at the tail wavelengths (350-400 nm) of the derCoum films was higher than with Coum films. This increased absorption is believed responsible for the slight narrowing of the fluorescence bandwidth. Similar results were obtained for the films at other concentrations. The absorption spectra of the other silylated dyes are also similar, except that the bi-functionalized dyes had significantly higher molar absorptivities. The fluorescence spectra of the other silylated dyes had shifts in the fluorescence maximum (20 nm) and some variance in the bandwidth. Regardless, all the dyes absorbed in the 320 nm range and fluoresce near 450 nm. Such results indicate that silylation of laser dyes does not significantly effect the fluorescence capabilities of the dye.

The fluorescence spectra of the solvent samples and the sol-gel films were quite different even though they were measured at similar pH values. This indicates that sol-gel environment greatly affects the fluorescence emission of the dye.

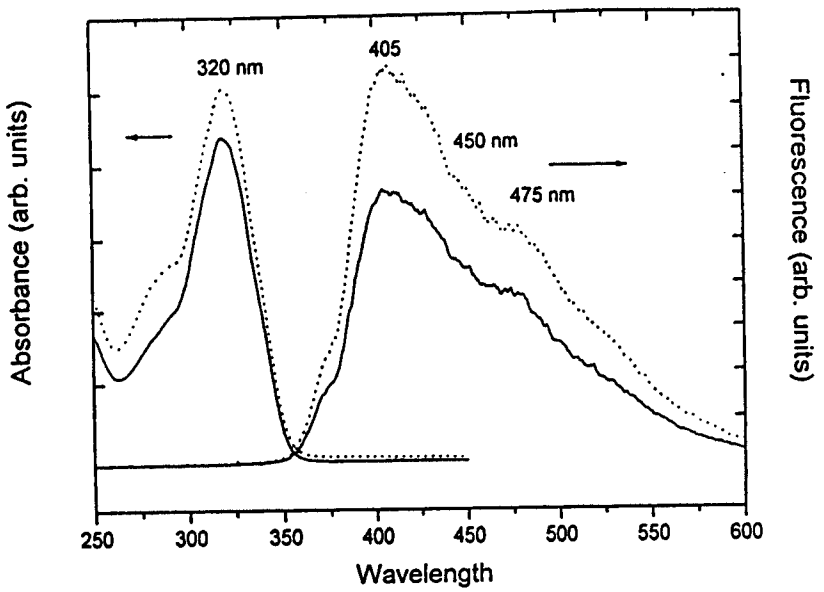

Fig. 6: Absorption and fluorescence curves of Coum (solid) and derCoum (dotted) in MeOH at pH 2.0.

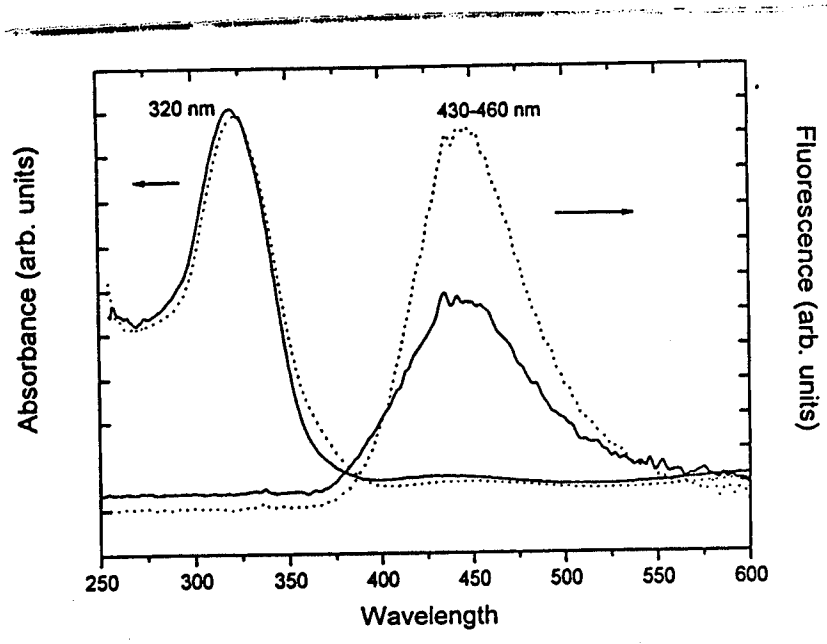

Fig. 7: Absorption and fluorescence curves of Coum (solid) and derCoum (dotted) in dried sol-gel silica films.

E. Fluorescence efficiency

The fluorescence quantum yield could not be measured quantitatively with the experimental setup used. The fluorescence efficiency can be described as the ratio of the number of photons emitted to the number of photons absorbed or as:

$$\phi_f = \frac{k_f}{k_f + k_{ic} + k_{isc}}$$

where k_f is the fluorescence rate constant, k_{ic} is the internal conversion rate constant, and the k_{isc} is the intersystem crossing rate constant. The relative fluorescence efficiency was determined for the sol-gel films by dividing the area of its fluorescence spectrum by the absorption at the excitation beam wavelength (337nm). Fig. 8 is a plot of this fluorescence efficiency as a function of concentration for the dye/sol-gel films. The fluorescence efficiency was higher for the derCoum films at all concentrations. In contrast, both Coum and derCoum in solvent had essentially the same fluorescence intensity, indicating that both have similar fluorescence efficiencies. The maximum in the fluorescence efficiency was observed at higher concentrations for the derCoum films (0.01 M) than for the

Coum films (0.001 M). The silylated dye film showed a 2 fold increase in the fluorescence efficiency at 0.01 M concentration with respect to the normal dye. This improvement is believed to be attributed to the greater rigidity of derCoum [reflecting a reduction of the internal conversion rate constant (k_{ic})], and greater dye isolation [reflecting a reduction of the intersystem crossing rate constant (k_{isc})].

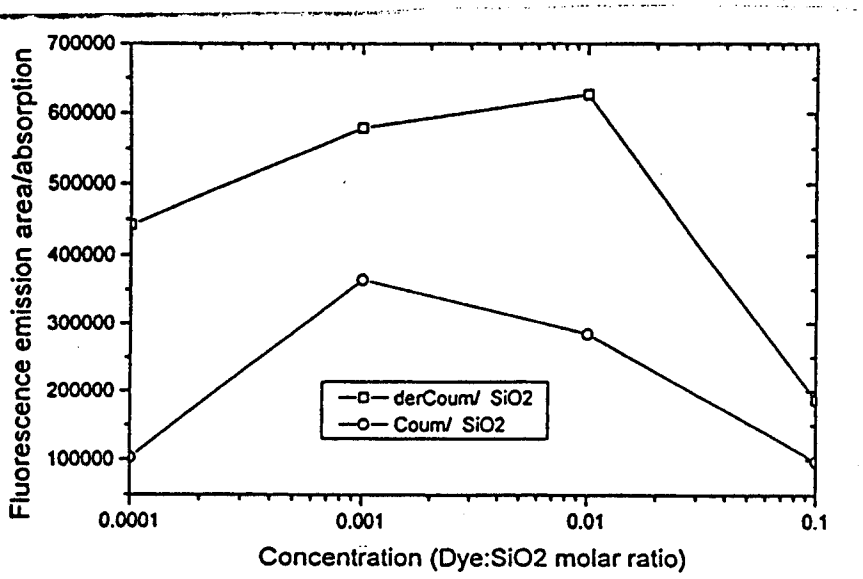

Fig. 8: Fluorescence efficiency as a function of concentration for dye doped films.

F. Dye extraction

To characterize the dye incorporation within the sol-gel matrix, dye extraction measurements were performed. The sol-gel films were soaked in THF at 50 C for several days. The THF was kept in an enclosed glass container, and

a reflux condenser was used to prevent loss of solvent by evaporation. The samples were periodically removed and the absorbance was measured at the absorption maximum wavelength.

Dye extraction experiments proved valuable in determining the degree of dye incorporation within the matrix. In Fig. 9, the absorption of the films (normalized to the film absorption before soaking) is plotted as a function of the soak time in THF. The derCoum sample did not show any decline in the absorbance after nearly 4500 min. This indicates that the dye is bonded to the SiO_2 matrix. In contrast, the Coum film showed a decrease in absorption of more than 80% within 1500 min of soaking, indicating substantial dye loss.

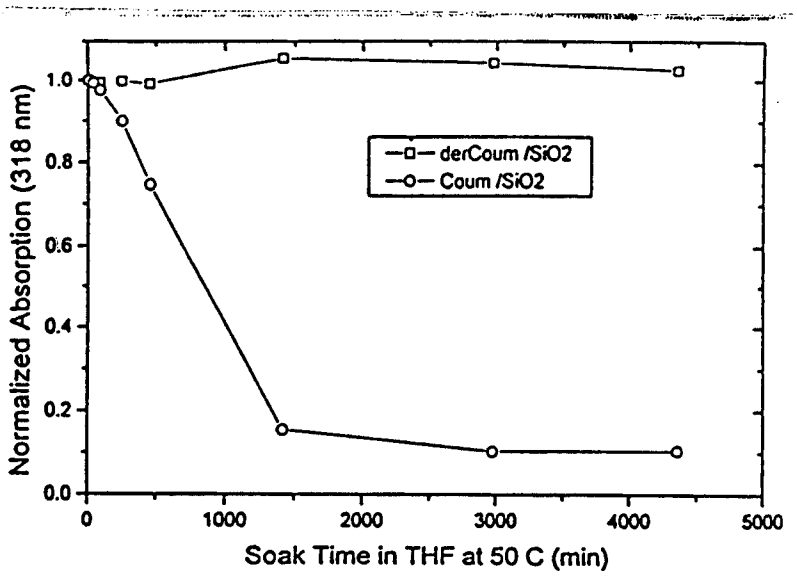

Fig. 9: Dye extraction of derCoum and Coum films.

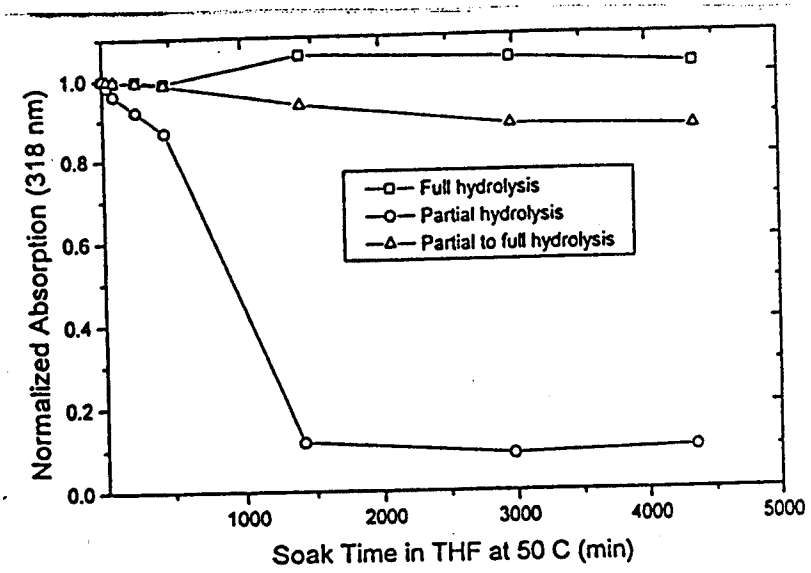

Fig. 10: Dye extraction of derCoum /SiO_2 films at various TMOS:H_2O ratios.

The leachability of the dye from its hosts depend significantly on the processing conditions (e.g., order of precursor mixing, hydrolysis time and water content). Prehydrolysis of the derCoum before mixing with TMOS resulted in films in which the derivatized dye could not be removed (Fig. 9). The water content also played a large role in the incorporation of derCoum within the sol-gel films (Fig. 10). Large dye loss occurred with a solution processed under partial hydrolysis (TMOS:H_2O=1:2), while no dye loss was observed with full hydrolysis (TMOS:H_2O = 1:4). For other conditions, where the solution was processed under

partial hydrolysis and additional water was periodically added to reach stoichiometric water content, slight dye loss was observed. The more permanent dye incorporation at high water content is attributed the greater hydrolysis of the dye and TMOS, resulting in greater condensation of the dye with the silica matrix.

In all variations of processing explored, the Coum dye was always almost completely extracted from the film within 1500 min of soaking. With solutions processed under full hydrolysis conditions, Coum was extracted more slowly than under partial hydrolysis conditions.

These results indicate that under proper processing conditions, the silylated dye can be incorporated within a sol-gel matrix to provide a more chemically stable material than with a normal dye. This allows for the incorporation of large concentrations of organic species while maintaining high chemical and environmental stability.

G. Photostability

Photostability is the most important property that was measured. Lack of photostability of laser dyes has been the chief factor that has prevented large scale commercialization of liquid and solid dye lasers. Photostability measurements were measured in a setup similar to the one shown in Fig. 4 except that the OMA was

replaced by a detector. The fluorescence output was monitored as function of the pump pulses. A typical photostability curve shown in Fig. 11 shows two distinct processes. Various experiments were performed to determine the nature of each process. From the data, the first process is a recoverable equilibration between the singlet and triplet states, while the second process is a permanent decay process. The permanent decay process represents the process in which the dye degrades. This is the property of concern to us. Therefore to compare samples, a photostability figure of merit has been defined as the normalized slope of long term process.

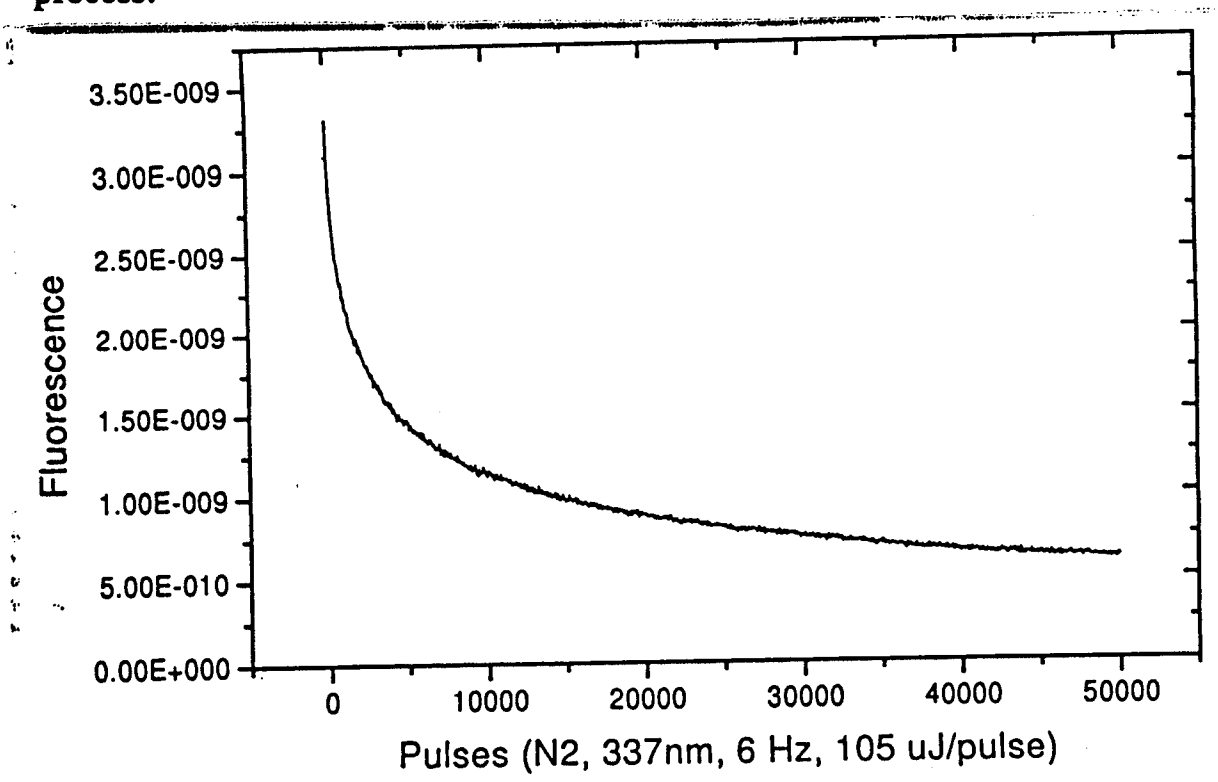

Fig. 11: A typical Photostability Curve

Under proper processing conditions (prehydrolysis times), the photostability of the silylated dye xerogels was found to be approximately 3 times better than its unsilylated counterpart (Table 1). Such results indicate a great advantage of using a silylated dye. Using the proper prehydrolysis times ensure high degree of dye bonding and caging by the silica matrix resulted in improved photostability.

Table 1: Photostability of Coum and DerCoum Xerogels

SAMPLE	Normalized Slope (10^{-6})
derCoum/SiO2 .05 M	-1.12
Coum/SiO2 .05 M	-3.44

N_2 Laser Pumping (337 nm, 1 mJ/cm^2, 6 Hz., 10 ns pulse, 0.10 cm^2 spot size)

H. Summary and Future Direction

Silylation of known laser dyes is attractive for many reasons. When used with sol-gel chemistry techniques, the silylated dye can participate in hydrolysis and condensation reactions, resulting in the dye to be chemically bonded to various host matrices as xerogels and Polycerams. Using a silylated Coumarin 4, higher

solubility was observed during sol-gel processing when compared with Coumarin 4. This provided ease of processing and the ability to achieve a higher dye concentration within the host. In xerogel hosts, the silylated dye was not extractable by a solvent, while the unsilylated dye was completely removed from the host. The silylated dye xerogel provides greater chemical and environmental stability. The optical properties of the silylated dye xerogels were also improved. The fluorescence efficiency improved 2-fold and the photostability improved 3-fold when compared with its unsilylated counterpart. Also, when both the silylated and unsilylated dye were examined in solvent, the absorption and fluorescence spectra were almost identical, indicating that chemical modification of the dye did alter the optical properties of the molecule itself.

Work is currently underway on measuring the optical properties of the other silylated coumarins dyes. Also, various hosts compositions are being examined and their effect on photostability. In addition, a new silylated laser dye (silylated Pyrromethene 567) is currently being synthesized. Pyrromethene laser dyes are inherently one of the most photostable laser dyes.

III. POLYCERAMS

A. Optical Properties of *Polyceramss* at Elevated Temperatures

Sol-gel techniques have been employed to synthesize organically modified hybrid materials (*polyceramss*) using functionalized polymers and metal alkoxides. When synthesized in the form of planar waveguides, these materials exhibit very low optical losses (<0.25 dB/cm), indicating a high level of homogeneity approaching the molecular level. The optical properties (index of refraction, thickness and optical attenuation) have been studied at temperature ranges of 25-100C. The ratio of the organic/inorganic content can be modified to obtain the desired dn/dT. Most importantly, the optical losses of the waveguides remain low despite temperature cycles.

The change in index of refraction as a function of temperature (dn/dT) is an important parameter in device performance. A large value of dn/dT can be severely detrimental to the optical performance of a given device. In addition, large changes in dn/dT may cause stress-related physical damage to the device during operation. Thus, knowledge of dn/dT for different waveguides is important in designing devices with minimal sensitivity to temperature fluctuations.

Sol-gel derived *polycerams* were synthesized using (N-triethoxysilylpropyl) O-polyethylene oxide urethane (MPEOU)* as a reactive functionalized polymer and Si and Ti alkoxides as inorganic components. *Polyceram* solutions were made by reacting tetraethoxysilane (TEOS) with H_2O (0.15 M HCl), titanium (IV) isopropoxide (TIP) and MPEOU. Solutions were spin-coated on rectangular (1 x 1.5 inches) fused silica substrates which were ultrasonically pre-cleaned in methanol. Spin-coating was conducted in a class 100 clean room using a Headway Spinner at a speed of 3000 rpm for 20 secs. Solutions were passed through a 0.1 μm syringe filter to reduce the number of adventitious particles in the films. The coatings were then dried in a vacuum oven for 72 hrs at 125C.

Standard prism-coupling techniques were used to obtain the index of refraction and thickness of the coatings by launching laser light into the TE_0 and TM_0 modes of the waveguides. The index of refraction and thickness can be obtained with good accuracy by measuring the coupling angles at the prism and fitting them using a theoretical dispersion curve. All waveguides were thick enough to support the first two modes (TE_0 and TM_0) at all temperatures. In addition, in a film of index $\underline{n}$, deposited on fused silica ($\underline{n_0}$), all guided modes (N_m) were in the

---

* Huls America, Piscataway

interval $n_0 < N_m < n$ at all temperatures. Measurements were conducted at the wavelength of 632.8 nm using a helium-neon laser.

A measure of the degree of condensation of the network can be obtained with index of refraction studies. Fig. 12 shows the measured vs. calculated index of refraction of MPEOU-SiO_2-TiO_2 as a function of weight % inorganic content. Calculcations are based on the simple rule of mixtures of the indices of MPEOU (n=1.495) and those of SiO_2-TiO_2 glass system with different mole ratios. The measured indices are only slightly lower than the calculated indices based on oxides. This suggests that the alkoxides of silicon and titanium were substantially converted to the oxides during processing- although the polarizability, e.g., of the TiOR and TiOH species may not be greatly different from that of TiO in a glass network.

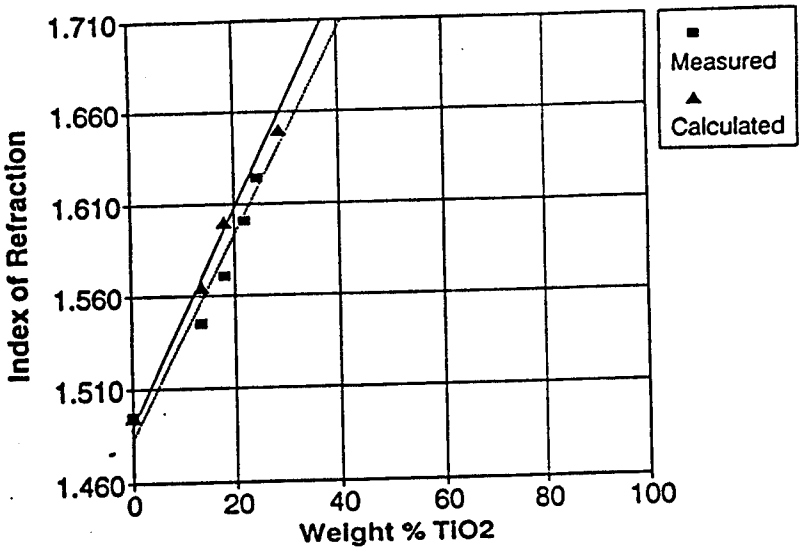

Fig. 12: Measured vs. Calculated Index of Refraction of MPEOU-SiO_2-TiO_2 *Polycerams* Plotted as a Function of Weight % TiO_2.

a. dn/dT Measurements

Heat treatment of waveguides was conducted using 3 heating resistors attached to the prism-coupling stage. Samples were heated for 1 hour prior to prism-coupling measurements to ensure temperature stability and uniformity along the film. In addition, waveguides remained heated at the desired temperature during prism-coupling experiments. Temperature studies were conducted in the range of 20°C (room temperature) to 100°C. Two measurements were taken at each temperature, and each cycle was repeated to ensure reproducibility of results.

Previous thermal analysis studies (TGA) indicated that MPEOU starts to decompose at 150°C, MPEOU-SiO_2 at 185°C, while MPEOU-SiO_2-TiO_2 does not start decomposing until 250°C. Hence, MPEOU-SiO_2-TiO_2 *polyceram* waveguides can withstand temperatures near 250°C. In this study, however, heating experiments were conducted only in the range of 20-100°C. To obtain the correct index of refraction of the *polyceram* waveguides at different temperatures, the refractive indices of the fused silica substrate and the prism were also calculated for various temperatures. The dn/dT of the fused silica substrate was approximated to have a value of 1.15×10^{-5} /°C in the linear regime of 20-100°C. The change of index vs. temperature of the prism (SFL6 glass), on the other hand, was not

linear in the temperature range of interest, and required the generation of a computer program.

Figure 13 exhibits the change in index of refraction of MPEOU-SiO_2-TiO_2 *polycerams* as a function of temperature. Linear fits through the plots indicate that the index of refraction decreases with increasing temperature for all four compositions.

The slopes of these linear fits yield the corresponding dn/dT's. Table 1 reports the calculated dn/dT's for the different compositions of MPEOU-SiO_2-TiO_2 *polycerams*. The values of dn/dT decrease with increasing TiO_2 content. Since the dn/dT's of organics are usually negative while those of inorganics are positive, as the amount of TiO_2 increases, the *polyceram* films with the same polymer content incorporate more of the oxide characteristics, thus resulting in lower dn/dT values. This indicates that to obtain waveguides with minimal dn/dT's, it is important to balance the organic to inorganic content and the chemistry condensation of the inorganic species (TiOH is known to condense more rapidly than SiOH; Ti is a recognized condensation catalyst for SiOH).

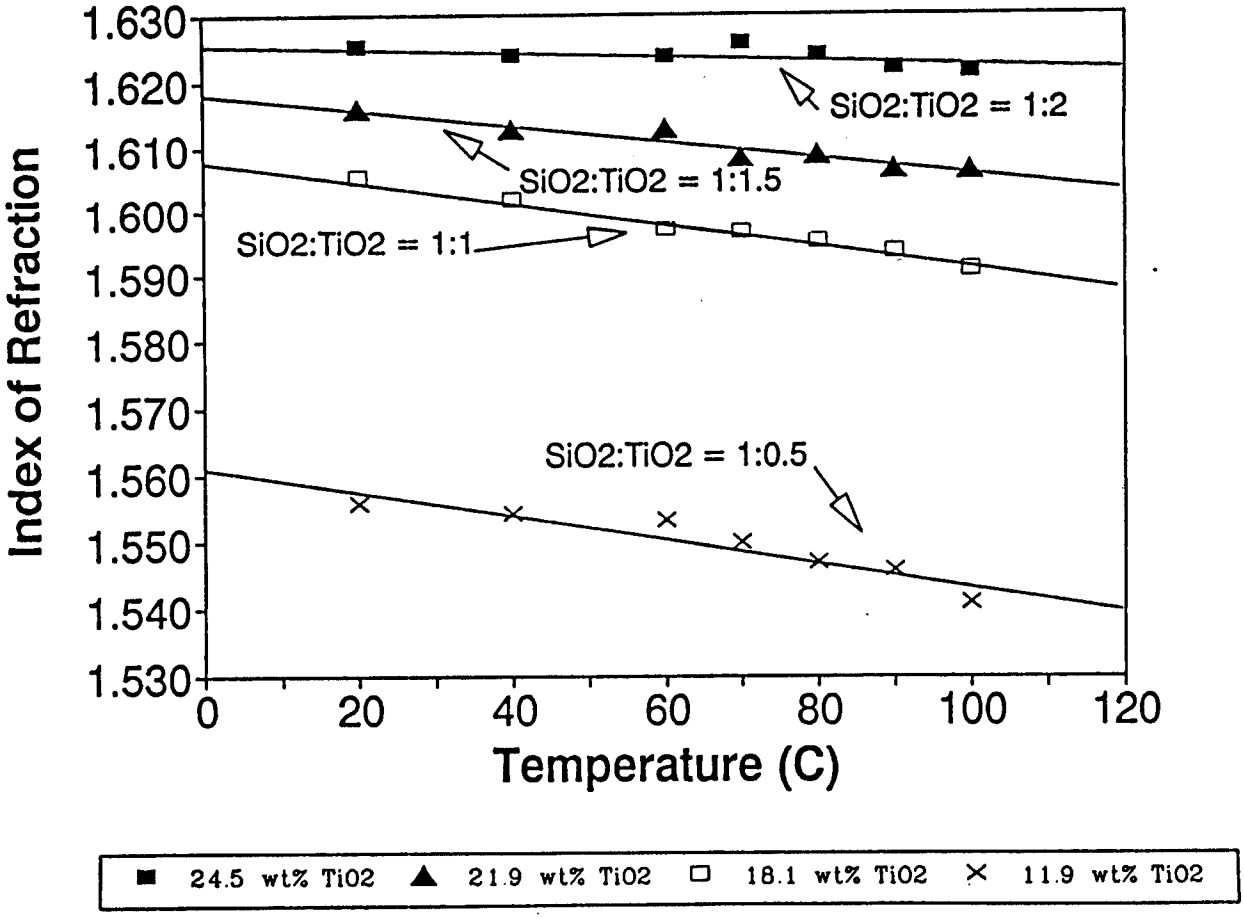

Fig. 13: Index of Refraction of MPEQU-SiO_2-TiO_2 *Polycerams* as a Function of Temperature (°C).

Weight % TiO_2 in MPEOU-SiO_2-TiO_2 *polycerams*	dn/dT (/°C)
11.9	-1.8×10^{-3}
18.1	-1.7×10^{-4}
21.9	-1.2×10^{-4}
24.5	-3.9×10^{-5}

Table 1: Measured Values of dn/dT for MPEOU-SiO_2-TiO_2 *Polycerams* as a Function of Weight % TiO_2.

Fig. 14 shows the thickness of the waveguides as a function of temperature in the above *polyceram* compositions. The thickness increases with increasing temperature. The thermal expansion of the polymer is larger than that of the inorganics. Hence, as the amount of TiO_2 increases, the change in thickness becomes smaller, again indicating that the *polyceram* incorporates more of the oxide characteristics. This finding is in agreement with the observed change in dn/dT with TiO_2 content.

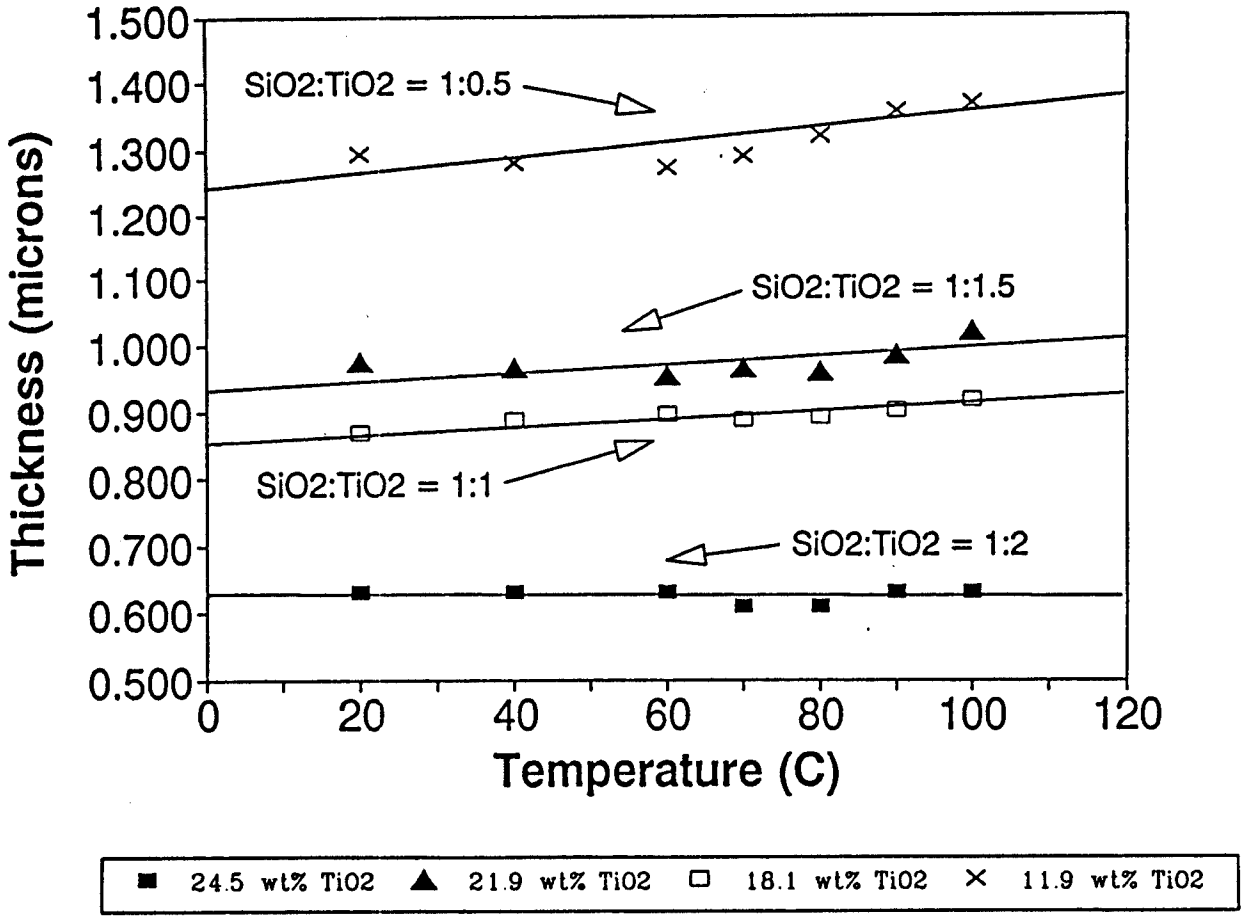

Fig. 14: Film Thickness (μm) of MPEOU-SiO_2-TiO_2 Polycerams as a Function of Temperature (°C).

All four waveguides were brought back to room temperature and re-measured. The index of refraction as well as the thickness of the films corresponded well with the values obtained prior to heating, thus indicating that the behavior is reversible.

b. Optical Attenuation Measurements

The optical losses of the waveguides were also determined at different temperatures. Fig. 15 shows the loss of a MPEOU-SiO_2-TiO_2 *polyceram* waveguide (SiO_2:TiO_2 mole ratio of 1:1) as a function of temperature. The loss remains constant until 125°C. The fluctuations are within experimental errors. A low loss is a result of total confinement of the excited mode within the guiding layer provided the layer is of high optical quality (high purity and homogeneity). Total confinement is dependent upon the Δn between the guiding layer and the substrate, as well the thickness of the guiding layer. It is therefore possible to obtain the same loss in a high index-low thickness waveguide as in a low index-high thickness waveguide. The constant attenuations in the MPEOU-SiO_2-TiO_2 *polyceram* indicate that although the index of refraction of the waveguide decreases with increasing temperature, the thickness increases, thus still confining the mode.

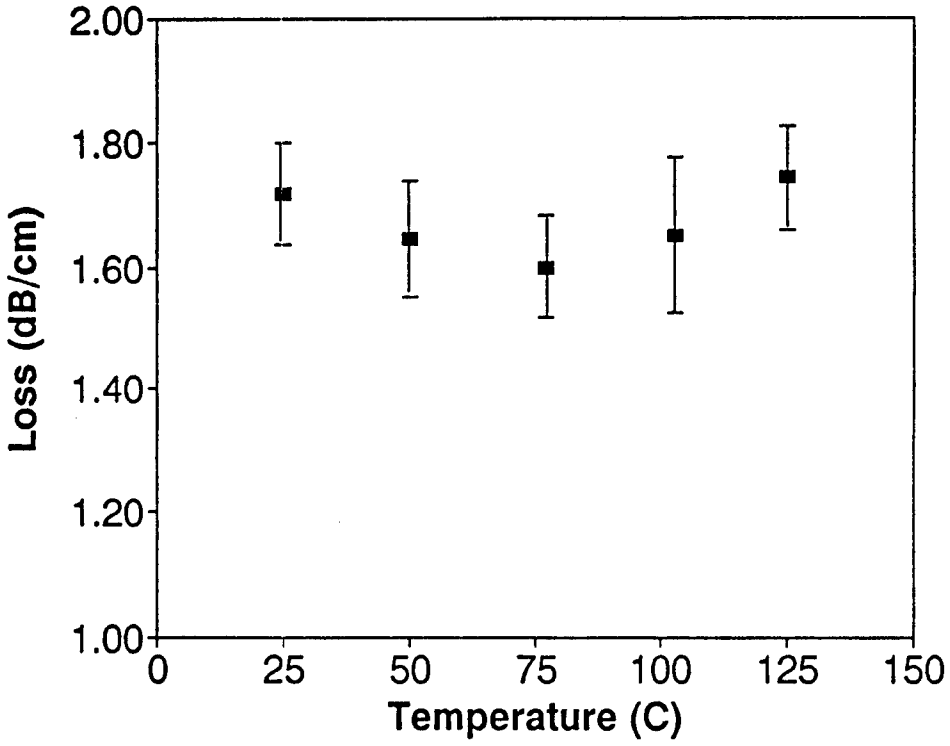

Fig. 15: Measured Optical Loss (dB/cm) of a MPEOU-SiO_2-TiO_2 (Si:Ti Mole Ratio of 1:1) Waveguide as a Function of Temperature (°C).

The above MPEOU-SiO_2-TiO_2 *polyceram* was held at 100°C for 72 hours, and the index of refraction and loss were measured at different intervals (Figs. 16 & 17). Both index of refraction and loss remained constant within this time interval. The fluctutations are within experimental errors. The waveguide was cooled back down to room temperature and re-measured. Again, no difference was obtained between the pre- and post-heating values.

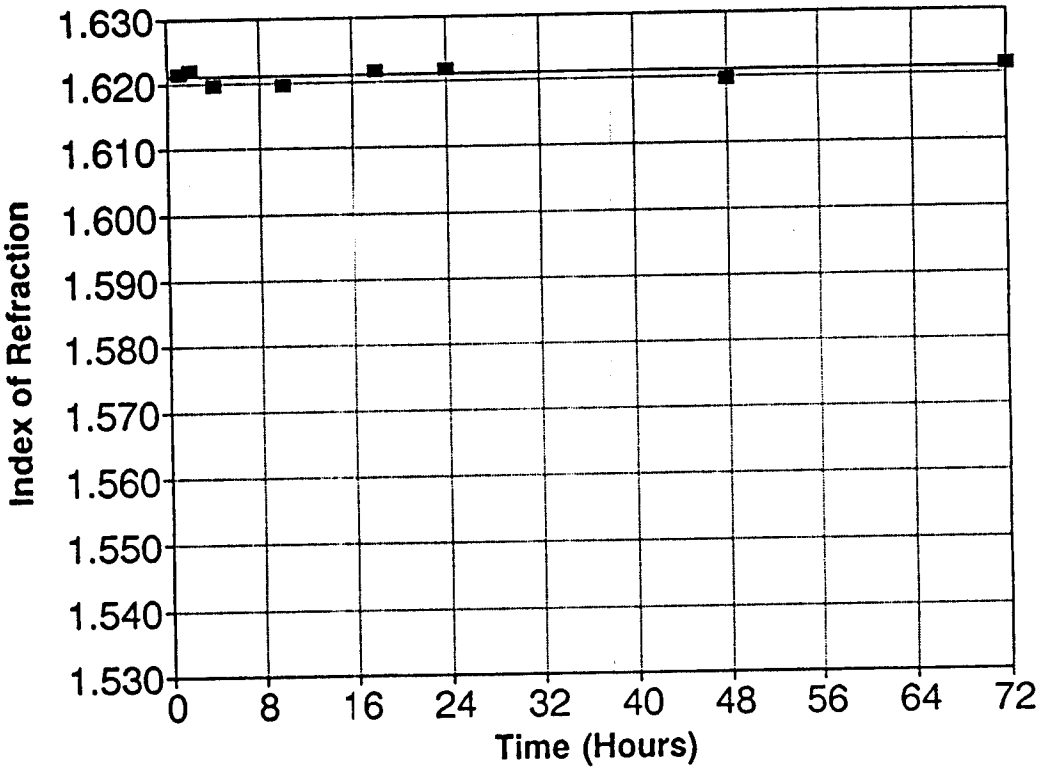

Fig. 16: Index of Refraction of a MPEOU-SiO_2-TiO_2 (Si:Ti Mole Ratio of 1:1) Waveguide as a Function of Time (hr).

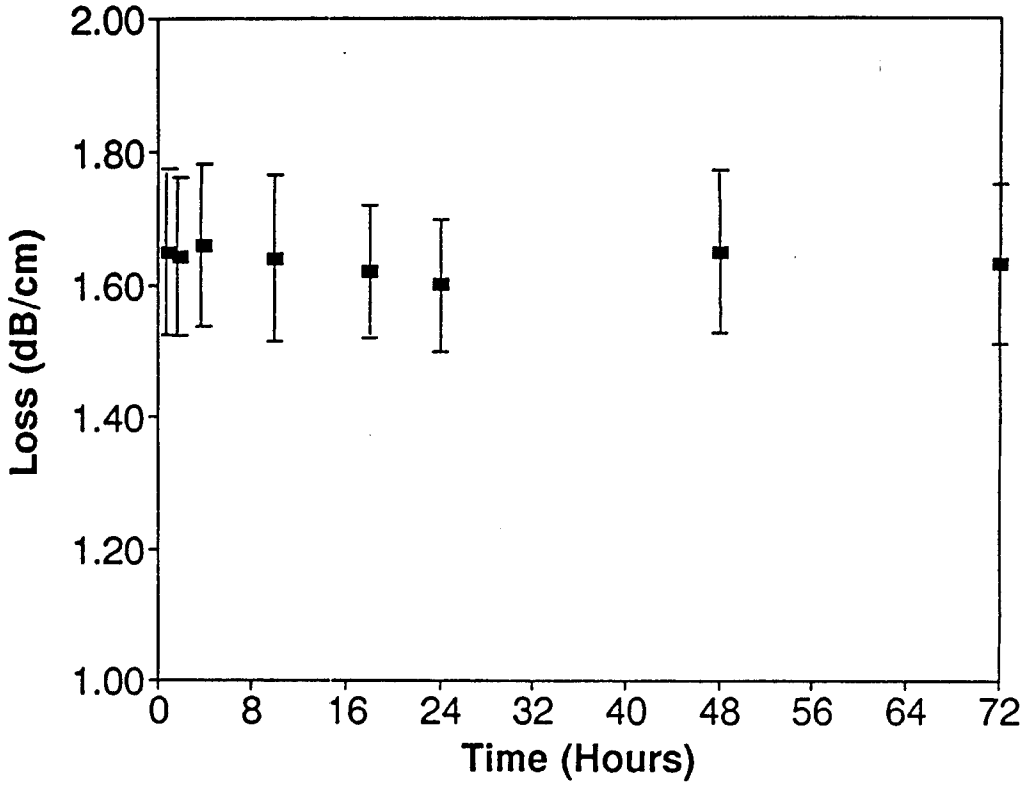

Fig. 17: Measured Optical Loss (dB/cm) of a MPEOU-SiO_2-TiO_2 (Si:Ti Mole Ratio of 1:1) Waveguide Heated to 100°C as a Function of Time (hr).

Measurements of the index of refraction and thickness of MPEOU-SiO_2-TiO_2 *polycerams* thus indicate that the chemistry of the waveguides can be easily altered through wet chemical techniques to yield compositions with minimal dn/dT. In addition, optical loss values remain insensitive to temperature up to more than

100°C. More importantly, these waveguides can withstand a temperature of 100°C for a minimum of 72 hours with no changes in index of refraction and loss. These results render *polycerams* attractive candidates for many passive or active optical devices.

B. Surface Patterning of *Polycerams*

Waveguide gratings have a multitude of applications in integrated optics, including uses as planar waveguide couplers, narrow-band filters, beam splitters, and focusing elements. Such gratings typically are fabricated by direct electron-beam writing or holography in combination with an ion-miling process. While these techniques are quite effective, they are not practical for mass-production purposes. Embossing into sol-gel thin films offers a practical non-vacuum method for the production of surface-corrugation gratings, as well as other integrated optic components. The embossing process consists of pressing a surface relief pattern (i.e. a diffraction pattern) into a gel film, thus producing a negative of the master on the film surface. We have found that despite the high organic content of our *polyceram* systems, surface gratings can be easily reproduced in *polycerams* with near-perfect feature replication.

a. MPEOU-SiO_2-TiO_2 *Polycerams*

So far, most surface embossing experiments have been conducted on the MPEOU-SiO_2-TiO_2 *polyceram* system. We have been able to emboss successfully sinusoidal patterns, channels and Y couplers of different sizes (5 μm, 50 μm and 100 μm) in MPEOU-SiO_2-TiO_2 *polyceram* films (Figs. 18, 19 and 20). In addition, we have been able to successfully emboss binary optic micro-lenses (Fig. 21). The reproducibility of the binary steps in the *polyceram* system is remarkable. In all the above cases, the depth of the embossed structures corresponds to 1/4 to 3/4 of the depth of the masters, with a near perfect replication of the width of the channels. Most importantly, we found that embossing in the MPEOU-SiO_2-TiO_2 *polyceram* system requires very few steps, making the art of fabrication of surface gratings in this system trivial and reproducible.

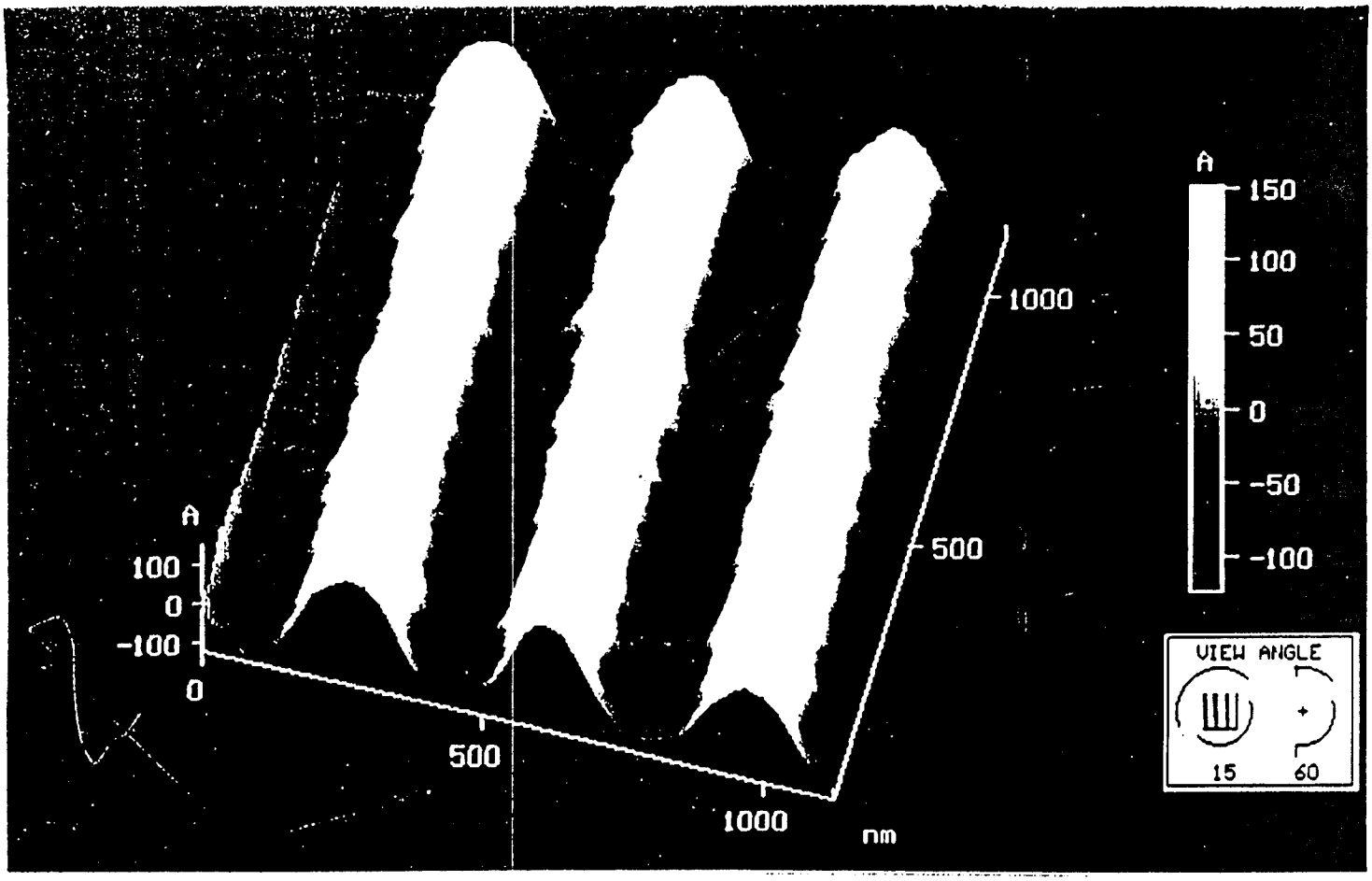

Fig. 18: Embossed Sinusoidal Pattern in the MPEOU-SiO_2-TiO_2 *polyceram* system.

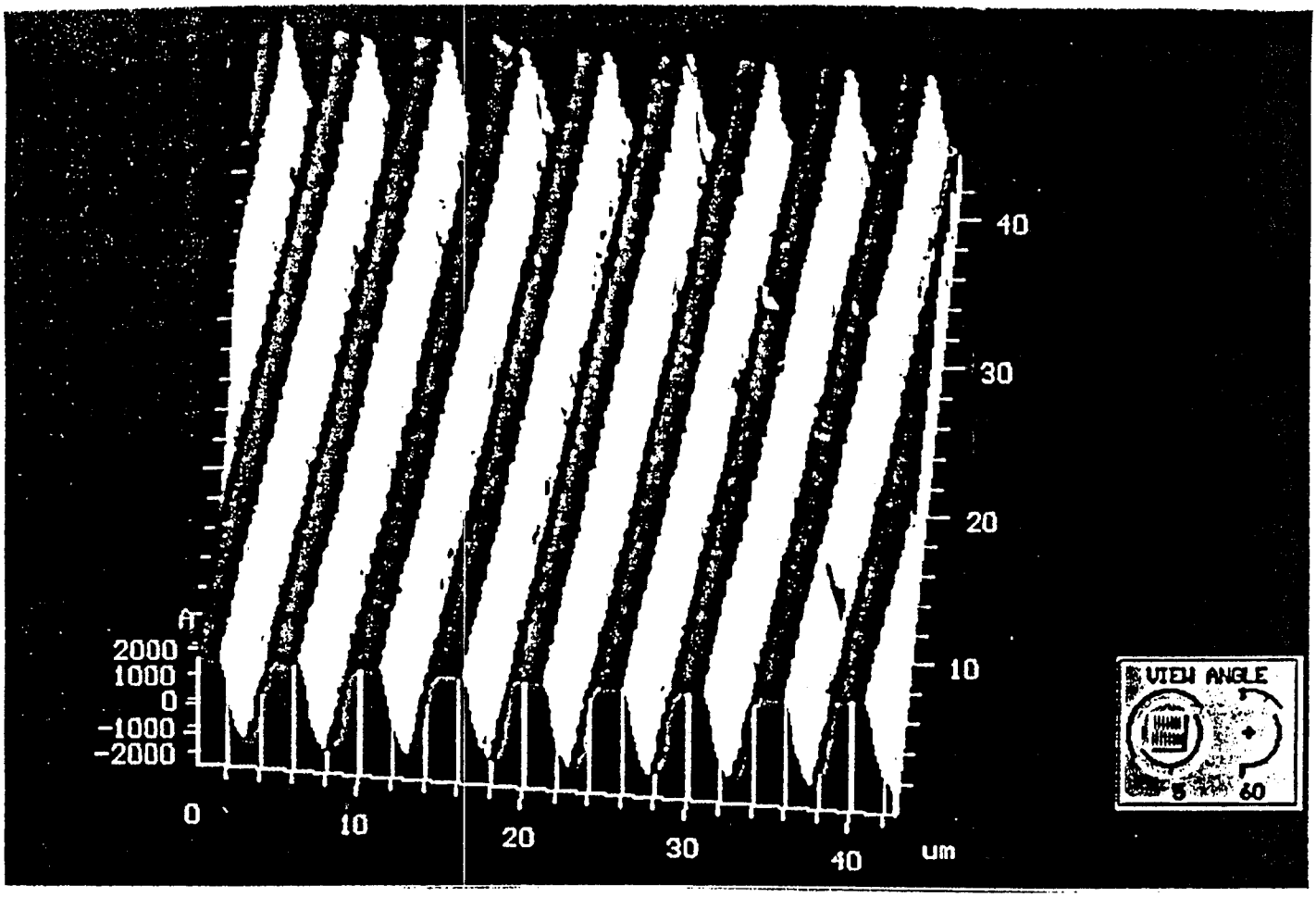

Fig. 19: Embossed Channel of 5 μm width in the MPEOU-SiO_2-TiO_2 *polyceram* system.

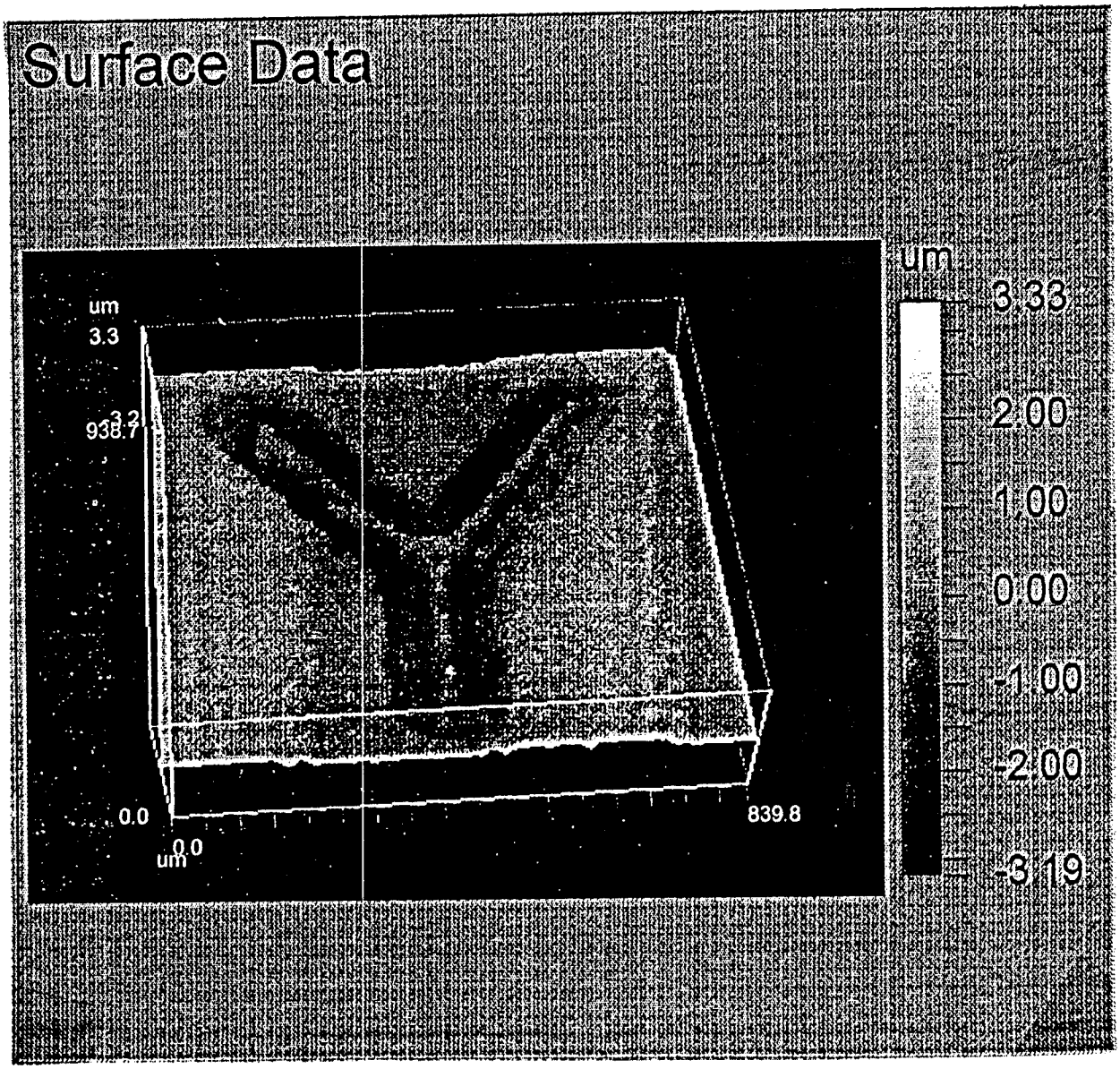

Fig. 20: Embossed Y beam-splitter in the MPEOU-SiO_2-TiO_2 *polyceram* system.

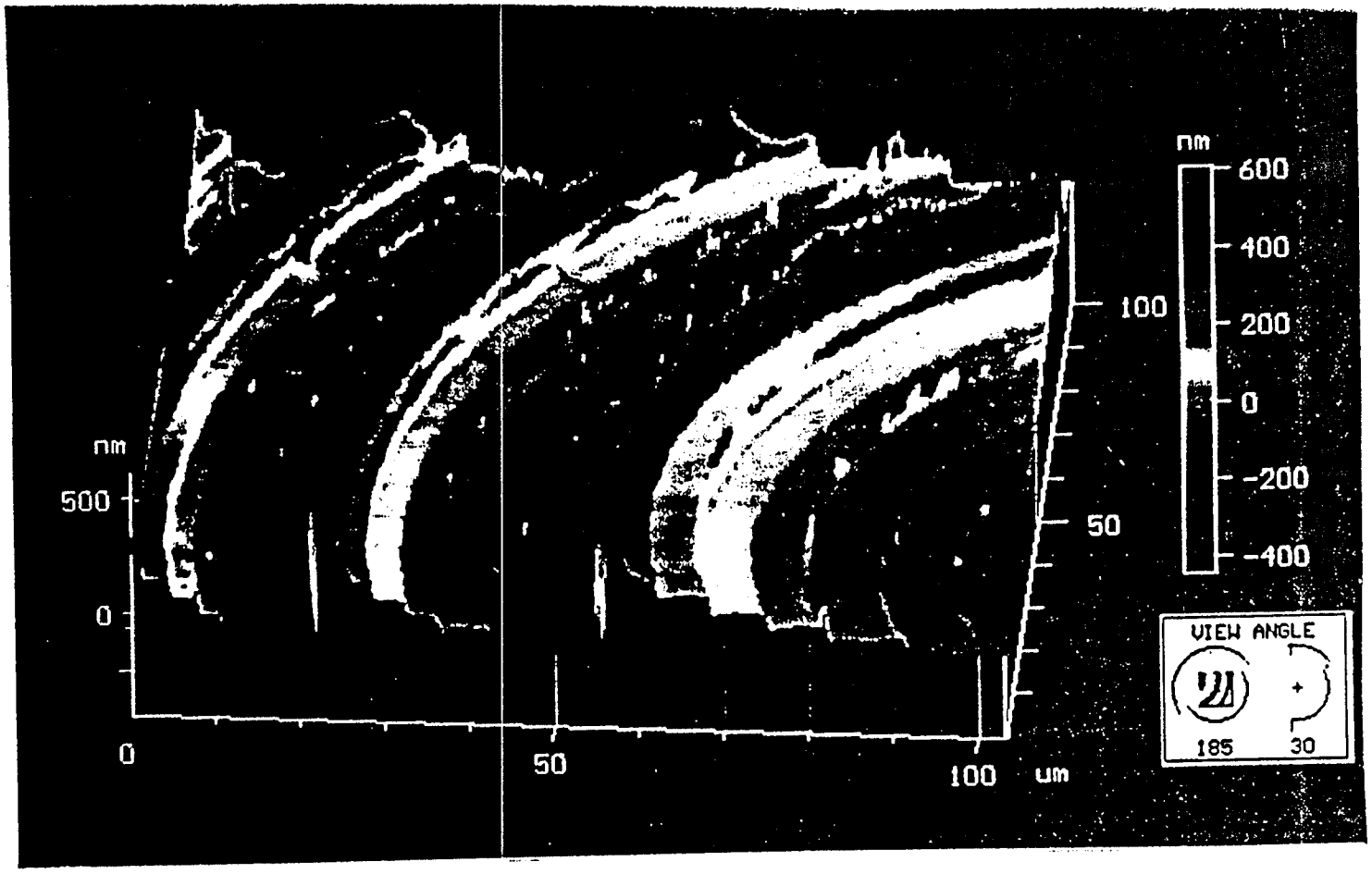

Fig. 21: Embossed 8-Level Binary-Optic Micro-Lens in the MPEQU-SiO_2-TiO_2 *polyceram* system.

b. PDMS *Polyceram* Systems

We have also expanded our surface embossing studies to investigate the embossing capabilities of the PDMS-SiO_2-TiO_2 and PDMS-SiO_2-ZrO_2 *polyceram* systems. Polydimethysiloxane (PDMS) is commercially more available and less expensive than N-triethoxysilylpropyl O-polyethylene oxide urethane (MPEOU). In addition, PDMS has a much simpler structure than MPEOU. Previous studies have shown that PDMS-SiO_2-TiO_2 and PDMS-SiO_2-ZrO_2 polyceram waveguides exhibit low optical attenuations (i.e. <0.15 dB/cm), and are therefore attractive candidates for embossing. In optimizing the embossing conditions to obtain well-defined replicated features, we found that, in contrast to the MPEOU *polyceram* systems, the best embossed gratings in the PDMS *polyceram* systems require pre-embossing heat treatments.

c. Masters

Embossed *polyceram* channels obtained from photoresist-coated masters are considerably cleaner and smoother than those produced from ion-milled masters. In addition, photoresist-coated masters produce deeper channels. It appears, therefore, that there is no need to increase the number of processing steps to eliminate the photoresist on the masters by ion-milling.

In a separate study, the embossing masters were coated with Diamond-Like-Carbon (DLC) in order to study the life expectancy of the masters. DLC appeared an attractive coating material due to properties such as chemical inertness, impermeability, smoothness and hardness. Embossing of the MPEOU-SiO_2-TiO_2 *polyceram* system, however, showed that DLC-coating of masters did *not* increase their life expectancy. Studies are currently underway to study the effects of including *fluorinating agents* in the *polyceram* chemistry to decrease the stickiness problems and increase the life expectancy of the masters.

Surface patterning of *polycerams* has been carefully optimized to turn this science into a mass-production technology with minimal number of processing steps and high reproducibility. In addition, embossing is not confined to only one *polyceram* system-it can be easily modified to successfully produce gratings in other *polyceram* systems as well (i.e PDMS-SiO_2-TiO_2 and PDMS-SiO_2-ZrO_2).